Ionics
DOI 10.1007/s11581-016-1953-1

ORIGINAL PAPER

Performance of developed natural vein graphite as the anode material of rechargeable lithium ion batteries

H. P. T. Sasanka Hewathilake[1] · Niroshan Karunarathne[1] · Athula Wijayasinghe[1] · N. W. B. Balasooriya[2] · A. K. Arof[3]

Received: 14 October 2016 / Revised: 1 December 2016 / Accepted: 19 December 2016

Abstract Electrochemical performance of natural vein graphite as an anode material for the rechargeable Li-ion battery (LIB) was investigated in this study. Natural graphite exhibits many favorable characteristics such as, high reversible capacity, appropriate potential profile, and comparatively low cost, to be an anode material for the LIB. Among the natural graphite varieties, the vein graphite typically possesses very high crystallinity together with extensively high natural purity, which in turn reduces the cost for purification. The developed natural vein graphite variety used for this study, possessed extra high purity with modified surface characteristics. Half-cell testing was carried out using CR 2032 coin cells with natural vein graphite as the active material and 1 M $LiPF_6$ (EC: DMC; vol. 1:1) as the electrolyte. Galvanostatic charge–discharge, cyclic voltammetry, and impedance analysis revealed a high and stable reversible capacity of 378 mA h g^{-1}, which is higher than the theoretical capacity (372 mA h g^{-1} for LiC_6). Further, the observed low irreversible capacity acquiesces to the high columbic efficiency of over 99.9%. Therefore, this highly crystalline developed natural vein graphite can be presented as a readily usable low-cost anode material for Li-ion rechargeable batteries.

Keywords Natural vein graphite · Lithium ion rechargeable battery · Anode material · Reversible capacity · Columbic efficiency

✉ Athula Wijayasinghe
athula@ifs.ac.lk; athulawijaya@gmail.com

H. P. T. Sasanka Hewathilake
tharindu.tsh@gmail.com

Niroshan Karunarathne
niroshan_ka@yahoo.com

N. W. B. Balasooriya
balasooriya@fas.seu.ac.lk

A. K. Arof
akarof@um.edu.my

[1] National Institute of Fundamental Studies, Hantana Road, Kandy, Sri Lanka

[2] Faculty of Applied Sciences, South Eastern University, Sammanthurai, Sri Lanka

[3] Center of Ionics, Faculty of Science, University of Malaya, 50603 Kuala Lumpur, Malaysia

Introduction

Since the introduction of rechargeable Lithium-Ion Battery (LIB), it became a leading rechargeable battery type due to its higher capacity, higher energy density, and very low self-discharge rate. Currently, LIB is the main energy source for most of the portable electronic devices, and there is a strong interest in utilizing LIB for electrical vehicles and grid storage systems [1]. In such critical applications Columbic efficiency should be maintained over 99%. However, there are number of unsolved materials related problems that restrict the development of the LIB as a cheaper and reliable portable power source [2, 3].

Graphitic materials are widely used for the anode of LIB. However, to minimize the electrolyte decomposition and subsequent surface film formation, the attention on anode components have moved towards the synthetic materials, oxide based compounds, and alloy composites [4–6]. Nevertheless, these advanced synthetic anode components attribute to the high cost, lower discharge capacity and large capacity losses.

Published online: 04 January 2017

In contrast, natural graphite exhibits many favorable characteristics, such as high reversible capacity, appropriate potential profile, and specially the low cost, to be an anode material for the LIB [7]. Though such favorable conditions are present, the large irreversible capacity loss during the first cycle, poor cycleability, and poor rate capability have limited its practical use. There are three modes of naturally occurring graphite namely, flake, vein, and amorphous graphite. Since the higher abundance throughout the world, majority of the studies are reported on investigation of flake graphite for the anode application of LIB [8–11]. However, compared with the natural formation, vein graphite possesses very high purity and high crystallinity in raw form than flake graphite. This provides much favorable conditions for vein graphite to be developed for LIB application.

Typically, natural vein graphite of Sri Lankan origin that exists in large reserves, contains about 95–98% of pure carbon, in the raw form. The formation of this vein graphite becomes very unique due to its morphological variations possessing different structural and physical characteristics [12]. Recent studies have indicated vein graphite to be promising anode material for the LIBs. Further, the investigations carried out on physical and chemical modification of vein graphite had also resulted in improving its electrochemical performance [13, 14]. Therefore, the present study was based on investigation of a selected morphological variety of natural vein graphite, which was already upgraded to ultra-high purity and surface modified, for anode application in LIB.

Materials and methods

Natural vein graphite (NVG) powder (particle size <53 μm) of Sri Lankan origin, that belongs to the "needle platy graphite" variety, was taken for this study. This selected graphite variety had already been subjected to simultaneous purification and surface modification through acid digestion technique, which uses a combination of HF, HNO_3, and H_2SO_4 acids. Prior to the cell assembling, this developed natural vein graphite (dNVG) was characterized with X-ray Diffraction (XRD) by "Rigaku-Ultima IV" X-ray diffractometer, using Cu-Kα_1 radiation (λ = 1.54 Å), Fourier Transform Infrared (FTIR) spectroscopy at 500–4000 cm^{-1} region by Nicolet 6700 spectrometer, Scanning Electron Microscopic (SEM) imaging with Energy Dispersive X-ray (EDX) spectroscopy (EEVO/LS 15 ZEISS), carbon content by ASTM 562 method, and d.c. electrical conductivity by four-probe technique.

Electrochemical characterization was conducted by assembling dNVG/$LiFP_6$/Li cell configuration with CR 2032 coin cell type. The coin cells were composed with graphite electrode (dNVG) and a lithium metal that were separated by a glass fiber film. The dNVG electrode was prepared by casting a mixture of 80% of active material (purified and surface modified Sri Lankan natural vein graphite), 15% of PVDF (Sigma Aldrich) binder, and 5% of acetylene carbon black (Sigma Aldrich) together with N-Methyl-2-pyrrolidone (NMP/Sigma Aldrich) solvent, on a copper current collector.

The tape cast electrodes were then dried at 120 °C for 24 h in a vacuum oven. 1 M $LiPF_6$ in ethylene carbonate and dimethyl carbonate (EC: DMC vol. 1:1/Sigma Aldrich) was used as an electrolyte. All the assembling procedures were conducted in argon filled glove box (Mbraun) by controlling the O_2 and water levels at less than 1 ppm level.

The charge–discharge tests were performed by using a battery testing system (Neware - CT3008) at a 0.2 C rate (1C = 372 mA h g^{-1}) within a cutoff voltage window of 0.002–1.50 V vs. Li/Li^+ at room temperature. Further, Cyclic Voltammetry (CV) analysis was conducted at 0–1.50 V with the scan rate of 0.1 mV/s (CH instrument electrochemical analyzer). The Electrochemical Impedance Spectroscopy (ESI) analysis was taken using "HIOKI 3522–50 LCR" analyzer with an amplitude of 0.1 V in the frequency range from 0.01 Hz to 100 kHz at the different states of the cell cycling. Impedance spectra were recorded at the potential of 0.90 V

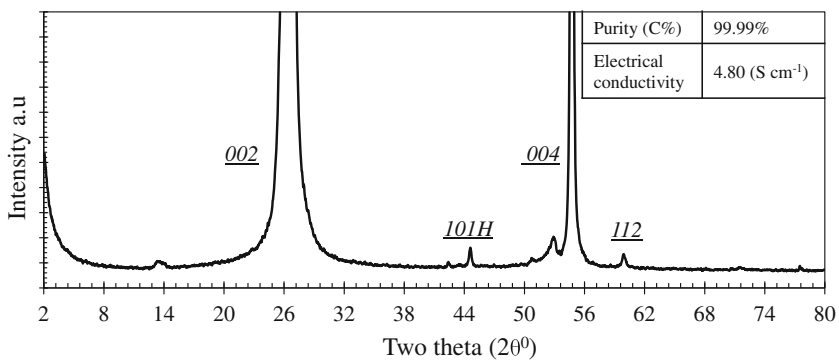

Fig. 1 X ray diffractogram of dNVG. *002*, *004*, *101*, and *112* are the common phases of crystalline graphite. The prefix "H" denotes the hexagonal phases of graphite

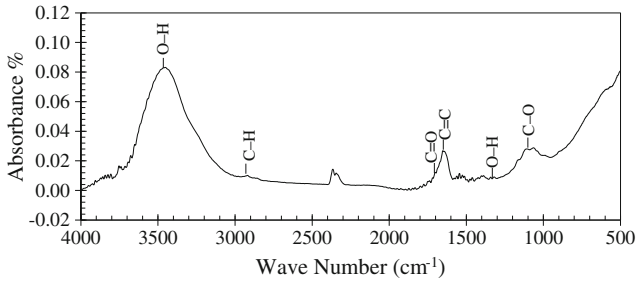

Fig. 2 FTIR spectra (KBr Pellets, Absorbance mode) for dNVG

Results and discussion

Material characterization

Figure 1 shows the X ray diffractogram obtained on the selected dNVG sample. The major crystallographic peaks of graphite, corresponding to (002) and (004) are appeared prominently in this diffractogram. It indicates that the purification and surface modification had not altered the structure of graphite. Further, it does not show any trace for impurity minerals in the diffraction pattern. In addition, this dNVG material possesses 99.99% of carbon content and the electrical conductivity of 4.80 S cm^{-1} at room temperature.

FTIR spectrum was obtained on dNVG to evaluate the effect of surface modification. As seen in Fig. 2, the FTIR spectrum evidences for the presence of vibrational bands corresponding to carbonyl groups $\nu_{C=O}$ stretching at 1720–1680 cm^{-1}, alkene groups $\nu_{c=c}$ stretching at 1637 cm^{-1}, and alcoholic groups $\nu_{O\text{-}H}$ stretching at 1360 cm^{-1} with high absorption values and $\nu_{c\text{-}o}$ stretching at 1260 cm^{-1} with a broad band. The presence of these peaks, which are related to acidic groups indicates the ability of the acid digestion technique to modify the surface of natural of graphite simultaneously with purification.

Figure 3 shows the SEM images obtained on the NVG (a) and dNVG (b) samples. The NVG has most contrast sharp thin edges and rough surfaces with impurity inclusions. After the treatment, the surface of dNVG become clearer and thin sharp edges converted to the rough edges with discontinuous steps. This appearance of dNVG proves the effective purification and surface modification by acid digestion method.

Discharge and charge profiles of Li/graphite cells

Figure 4 illustrate the initial discharge–charge profiles for the assembled dNVG/$LiFP_6$/Li half-cell at the current rate of 0.2 °C. The discharge curves drops down smoothly from 1.56 V to about 0.2 V, where the first lithium intercalation initiates, and it indicates the absence of strong passivation reaction (see Fig.4a). Moreover, a slight plateau, "plateau a" appears in about 0.72 V, provides evidences for the formation of the SEI layer (see Fig.4b).

Commonly, in the graphite electrode, the intercalation process occurs through a stage mechanism with the reversible formation of well-identified lithium-graphite intercalation compounds. Here, the lithium ions are gradually inserted between single graphite layers and a maximum of one lithium per six carbons (LiC_6) is expected to be intercalated, under ambient conditions, in the van der Waals gaps above and below a carbon hexagon. This is related to a 372 mA h g^{-1} of specific theoretical capacity. This intercalation occurs only at the prismatic plane of graphite, and it is possible through the basal plane only at defect sites. The graphite structure undergoes several characteristic staged phase transformations as the amount of lithium intercalation increases [15]. The characteristic stage formation during lithium intercalation into graphite is a stepwise process.

The lithiation–delithiation process of the cell in Fig. 4b reveals five stages of the lithiation in graphite electrode at the voltage below of 0.2 V vs. Li/Li^+. These stages may be attributed for the five continuous phase transitions starting from LiC_{72} and undergoes though LiC_{36}, LiC_{27}, LiC_{18}, LiC_{12}, up to LiC_6 [16].

Moreover, the discharge curve of untreated natural vein graphite (NVG) has two additional plateaus that correspond to reduction of solvents or contaminants (1.45 V vs. Li/Li^+) and graphite exfoliation (~0.5 V) [14]. Notably, after chemical purification, those peaks have been disappeared due to the possible stabilization of the structure of natural vein graphite without contaminations. The formation of SEI layer prevents solvent co-intercalation with lithium into the graphite, which causes the exfoliation of the graphite sheets.

Figure 4c shows the resultant high reversible capacity (378 mA h g^{-1}) with low irreversible capacity (53 mA h g^{-1}) for the first discharge–charge profile. This is

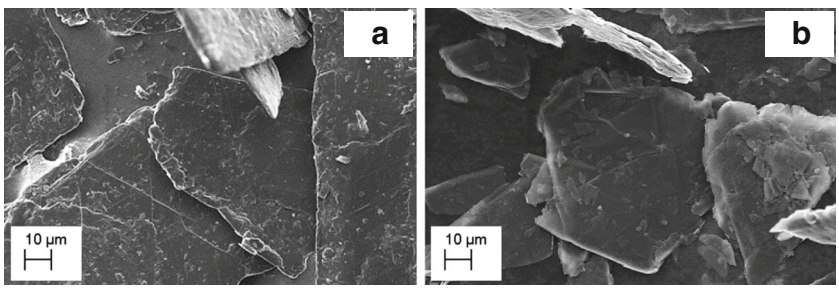

Fig. 3 SEM images under 20 kW of raw NVG (**a**) and dNVG (**b**)

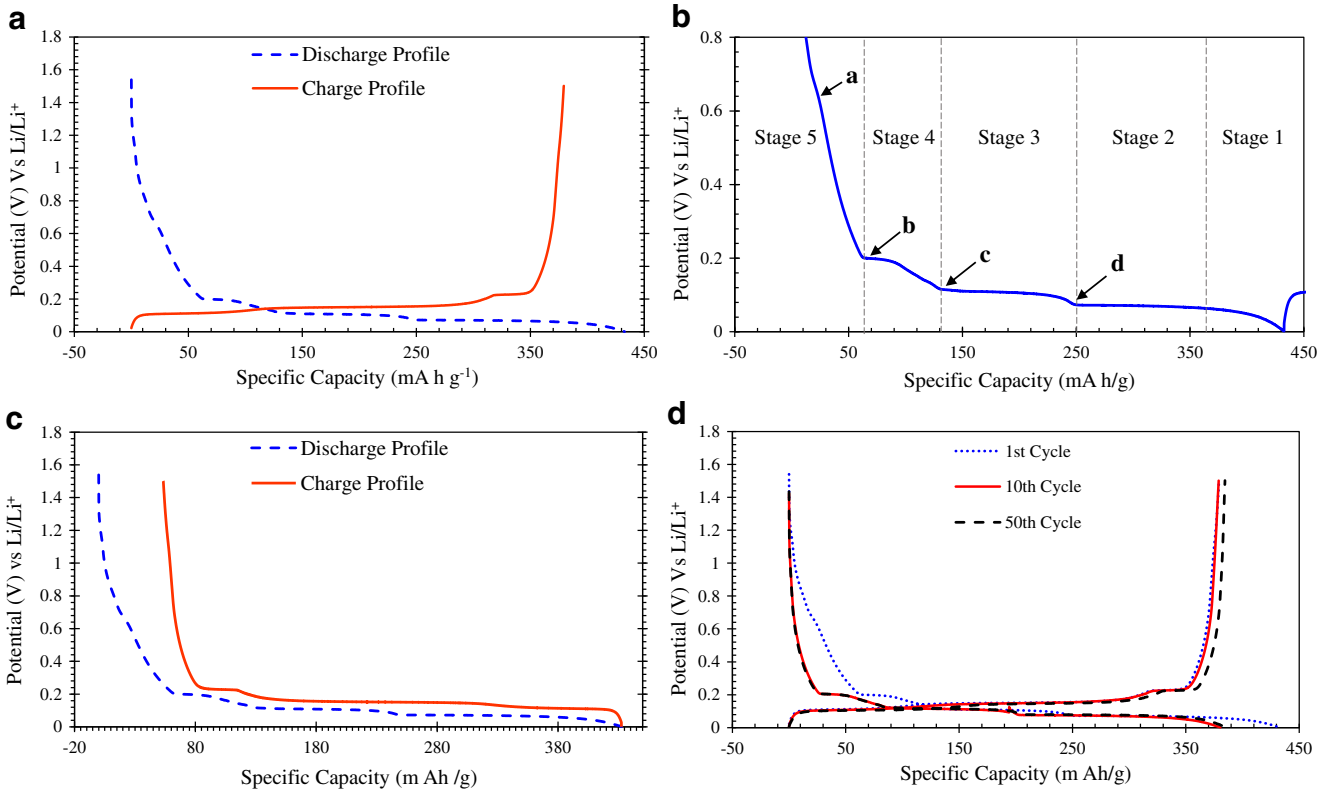

Fig. 4 **a** Discharge and charge profiles in the first cycle of dNVG. **b** Lithiation–delithiation of first discharge. **c** reversible and irreversible capacity, and **d** Comparison of the 1st-10th-50th charge discharge cycles

interestingly a low irreversible capacity and a high reversible capacity compared to the commercial LIB. The absence of the strong passivation reactions and formation of the SEI layer could have limited the capacity loss to 14%.

Figure 4d compares the 1st, 10th, and 50th cycles charge–discharge profiles. Though a deviation is appeared due to the irreversible capacity loss seen in between 1st and 10th cycle discharge, the 10th and 50th cycles discharge curves coincide with each other, providing evidences on the reversible capacity at 378 mA h g^{-1}.

Figure 5a shows the constant current discharge at 0.2 C rate throughout the first 50 cycles. In galvanostatic charge–discharge of Li-ion half-cell with dNVG anode, it tends to form LiC_6 intercalation, which gives a theoretical capacity of 372 mA h g^{-1}. The previous studies on vein graphite are reported reversible capacity considerably less than the theoretical capacity, at very low current rates [14, 16]. However, the dNVG used in this study shows a considerably higher capacity (378 mA h g^{-1}) at a relatively high current rate of 0.2 C, without considerable fading of the reversible capacity.

Further, half-cell performance for the dNVG was taken at different current rates of 0.2, 0.5, 1, and 2 C and they are illustrated in Fig. 4b. A capacity fade can be observed with the increasing of current rate, and it could be due to the IR drop of the cell. However, as Fig. 5b demonstrates the application of the same initial current rate of 0.2 C even after adapting the rate at 2 C, the same reversible capacity of 378 mA h g^{-1} was resulted without any fading. This behavior confirmed that the internal resistance of the cell has not adversely affected the cycling performance.

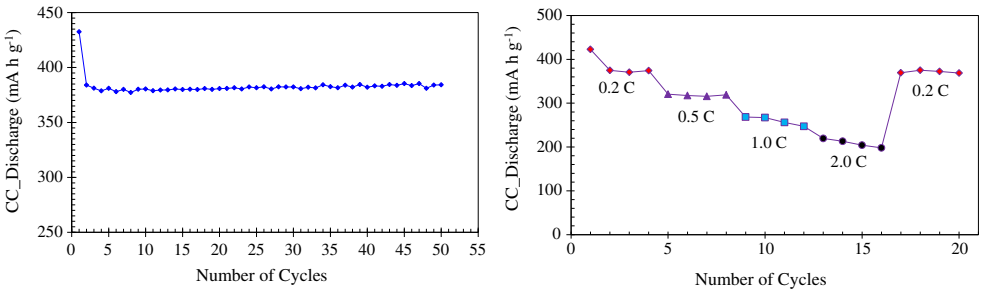

Fig. 5 **a** Cycle profiles of dNVG anode at charge–discharge rate of 0.2 C and **b** cycle profiles of dNVG at different current rates of 0.2, 0.5, 1, and 2 C

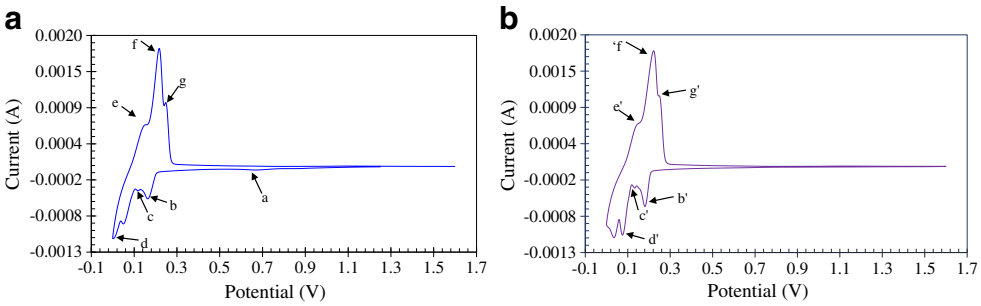

Fig. 6 The cyclic voltammograms obtained for the half cell containing dNVG electrode at a rate of 0.1 mV/s. **a** first voltammogram cycle and **b** second voltammogram cycle

Enhancement of the purity and surface modification by chemical oxidation can produce surface films that may stabilize the crystalline structure of graphite and hence increase the reversible capacity [17]. Similarly, the possible formation of nano channels on surface of graphite, as a result of surface modification, could provide extra pathways merely for the Li ion diffusion. That can ease the lithiation and delithiation process, hence, a longer life can be obtained for the anode without considerable capacity fading. The enhanced performance, especially of the high reversible capacity with minimal fading, observed in this study, could directly be related to those important characteristics inherent with the purified and surface modified NVG powder used for this study.

Cyclic voltammetry analysis of Li/graphite cells

Cyclic voltammogram study of the half cell (dNVG/LiFP6/Li) was carried out at a rate of 0.1 mV/s, and the resulted voltammograms are shown in Fig. 6. This CV study further confirms the existence of the reduction peaks identified in the galvanostatic study. As seen in Fig. 6a, a broad peak marked as "a" recorded at around 0.7 V confirms the formation of SEI layer during the first cycle [14]. In the low potential region of the first cycle discharge, three significant peaks of lithiation can be seen below 0.2 V. They are appeared at the potential values of 0.16 V (peak b), 0.12 V (peak c), and 0.05 V (peak d) vs. Li/Li^+. All these three peaks are corresponding with the same series of reversible peaks appeared at 0.15 V (peak e), 0.22 V (peak f), and 0.26 V (peak g) vs. Li/Li+, which represent the delithiation process. The second cycle of the voltammogram taken at the same rate of 0.1 mV/ is shown in Fig. 6b. It contains all the lithiation and delithiation peaks as observed with the first cycle. However, in the second cycle, there is not any peak to be observed corresponding to the SEI layer formation.

Electrochemical impedance analysis of Li/graphite cell

The electrochemical impedance spectroscopy was performed in the frequency range from 0.01 Hz to 100 kHz for the half cell containing dNVG electrode. The Nyquist complex impedance plots obtained before cycling and while the cycling in progress are shown in Fig. 7. According to Fig. 7, a semi-circle of a large diameter is reported for the half-cell before cycling, and it can be attributed to the formation of SEI layer on the dNVG electrode. However, the diameter of the semi-circle decreases with the cycling in progress, indicating lowering of the impedance. It explains that Li^+ ion diffusion becomes easier with the formation of this SEI layer with possible enhancement of ionic conductivity of the cell. Notably, all the semi-circles are started at the same point and that evidences for the stability of the electrolyte during charging-discharging process.

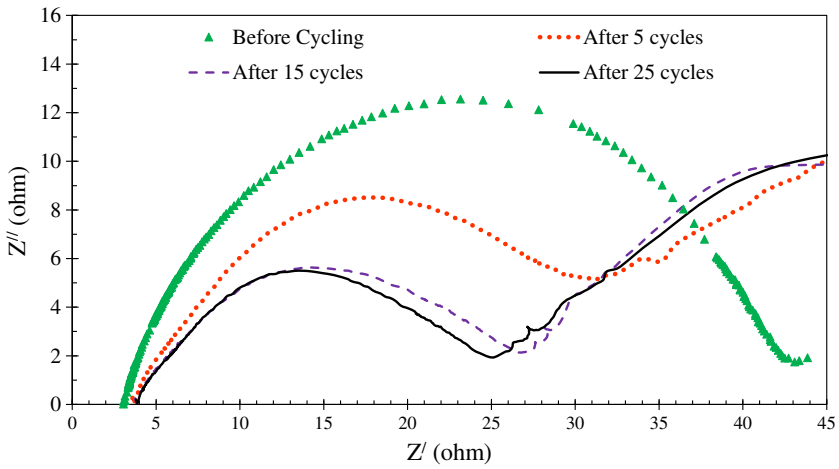

Fig. 7 Nyquist complex impedance plot obtained on the half-cell assembled with dNVG electrode

Conclusion

The developed natural vein graphite variety used for this study possess characteristics such as extra high purity (99.99%), adequate electrical conductivity, modified surface, and high crystallinity, desirable for the anode application in Li-ion rechargeable batteries. Cyclic voltammograms and the charge–discharge studies revealed a high stable reversible capacity of 378 mA h g^{-1}, which is significantly higher than the theoretical capacity (372 mA h g^{-1} of LiC_6). Also, the resulted low irreversible capacity acquiesces to the high Columbic efficiency of over 99.9%. Moreover, the formation of SEI layer without strong passivation reaction, smooth lithiation–delithiation process without structural exfoliation and solvent co-intercalation were well evidenced by the first cycle charge–discharge curves and cyclic voltammograms. Further, the galvanostatic cycling profiles obtained at a constant current rate as well as at different current rates proved the structural stability and the low internal resistance of the developed natural vein graphite used for this study. In addition, the electrochemical impedance analysis importantly attested the formation of SEI layer supporting unperturbed Li^+ ion diffusion due to possible enhancement in ionic conductivity when cycling in progress. Altogether, this study revealed the fact that highly crystalline natural vein graphite is a suitable low-cost alternative anode material for the Li-ion rechargeable batteries.

Acknowledgements Financial assistance by the Innovative Research Grant −2013 of University Grant Commission (UGC), Ministry of Higher Education, Sri Lanka and MOSTI – NANOTEKNOLOGI TOP-DOWN (NANOFUND), Grant No. 53-02-03-1089 are highly acknowledged. Authors would like to thank Mr. M.Z. Kufian and Prof. M.A. Careem from the Center of Ionics, Faculty of Science, University of Malaya for the guidance, laboratory facilities and fruitful discussions.

References

1. Whittingham MS (2004) Lithium batteries and cathode materials. Chem Rev 104:4271–4301
2. Samarasingha P, Wijayasinghe A, Behm M, Dissanayake L, Lindbergh G (2014) Development of cathode materials for lithium ion rechargeable batteries based on the system Li(Ni1/3Mn1/3Co(1/3-x)mx)O2, (M = Mg, Fe, Al and x = 0.00 to 0.33). Solid State Ionics 268:226–230
3. Samarasinghe P, Nguyen D, Behm M, Wijayasinghe A (2008) Electrochemical behavior and material characteristics of Li(Ni1/3Co1/3Mn1/3)O_2 synthesized by Pechini method for positive electrode in Lithium Ion battery. Electrochim Acta 53:7995–8000
4. Teo LP, Buraidah MH, Arof AK (2015) A novel LiSnVO4 anode material for lithium-ion batteries. Ionics 21:2393–2399
5. Park MS, Lee J, Lee JW, Kim KJ, Jo YN, Woo SJ, Kim YJ (2013) Tuning the surface chemistry of natural graphite anode by H3PO4 and H3BO3 treatments for improving electrochemical and thermal properties. Carbon 62:278–287
6. Wang H, Yoshio M (2001) Effect of iodine treatment on the electrochemical performance of natural graphite as an anode material for lithium-ion batteries. J Power Sources 101:35–41
7. Wang H, Ikeda T, Fukuda K, Yoshio M (1999) Effect of milling on the electrochemical performance of natural graphite as an anode material for lithium-ion battery. J Power Sources 83:141–147
8. Guo H, Li X, Wang Z, Peng W, Guo Y (2005) Mild oxidation treatment of graphite anode for Li-ion batteries. J Cent S Univ Technol 12:50–54
9. Lu XJ, Forssberg E (2002) Preparation of high-purity and low-Sulphur graphite from Woxna fine graphite concentrate by alkali roasting. Miner Eng 15:755–757
10. Wu YP, Rahm E, Holze R (2003) Carbon anode materials for lithium ion batteries. J Power Sources 114:228–236
11. Wu YP, Jiang C, Wan C, Holze R (2002) Modified natural graphite as anode material for lithium ion batteries. J Power Sources 111: 329–334
12. Touzain P, Balasooriya N, Bandaranayake K, Descolas-Gros C (2010) Vein graphite from the Bogala and Kahatagaha–Kolongaha mines, Sri Lanka: a possible origin. Can Mineral 48: 1373–1384
13. Balasooriya NWB, Touzain P, Bandaranayake PWSK (2007) Capacity improvement of mechanically and chemically treated Sri Lanka natural graphite as an anode material in Li-ion batteries. Ionics 13:305–309
14. Balasooriya NWB, Touzain P, Bandaranayake PWSK (2006) Lithium electrochemical intercalation into mechanically and chemically treated Sri Lanka natural graphite. J Phys Chem Solids 67: 1213–1217
15. Dresselhaus MS, Dresselhaus G (2002) Intercalation compounds of graphite. Adv Phys 51(1):1–186
16. Zhang S, Ding MS, Xu K, Allen J, Jow TR (2001) Understanding solid electrolyte interface film formation on graphite electrodes. Electrochem Solid State Lett 4(12):206–208
17. Amaraweera THNG, Balasooriya NWB, Wijayasinghe, HWMAC, Attanayaka ANB, Dissanayake MAKL, Mellander BE (2014) Development of Sri Lankan natural vein graphite as anode material for lithium-ion rechargeable batteries. 14th Asian Conference on Solid State Ionics 252–259. doi:10.3850/978-981-09-1137-9_039